# Development of a WDM platform for charged-particle stopping experiments

**AB Zylstra[1,2], JA Frenje[1], P E Grabowski[3], C K Li[1], G W Collins[4], P Fitzsimmons[5], S Glenzer[6], F Graziani[4], S B Hansen[7], S X Hu[8], M Gatu Johnson[1], P Keiter[9], H Reynolds[5], J R Rygg[4], F H Séguin[1] and R D Petrasso[1]**

[1] Plasma Science and Fusion Center, Massachusetts Institute of Technology, Cambridge, MA 02139; [2] Los Alamos National Laboratory, Los Alamos, NM 87544; [3] University of California Irvine, Irvine, CA 92697; [4] Lawrence Livermore National Laboratory, Livermore, CA 94550; [5] General Atomics, San Diego, CA 92186; [6] SLAC National Accelerator Laboratory, Menlo Park, CA 94025; [7] Sandia National Laboratories, Albuquerque, NM 87185; [8] Laboratory for Laser Energetics, Rochester, NY 14623; [9] University of Michigan, Ann Arbor, MI 48109

E-mail: zylstra@lanl.gov

**Abstract**. A platform has been developed for generating large and relatively quiescent plasmas in the warm-dense matter (WDM) regime on the OMEGA laser facility. A cylindrical geometry is used to allow charged-particle probing along the axis. The plasma heating is radiative by L-shell emission generated on the outside of the cylinder. The cylinder drive is characterized with x-ray diagnostics. Possibilities for direct characterization of the plasma temperature are discussed. Finally, the unimportance of electromagnetic fields around the target is demonstrated with proton radiography. We expect this platform to be used extensively in future experiments studying charged-particle stopping in this regime.

## 1. Introduction

The stopping of charged particles has been studied extensively over the last century, in both cold material[1], and in plasmas[2]. Plasma theory is challenging in high-density regimes, where the Coulomb logarithm becomes small, and degeneracy and/or strongly-coupled plasma effects can become important. However, several theories have been developed[3, 4, 5]. The stopping power in this regime is a fundamental test of dense plasma physics, and relevant to the realization of laboratory-scale thermonuclear fusion, where $\alpha$ bootstrap heating occurs via charged-particle stopping. Several recent novel experiments have measured charged-particle stopping in dense plasmas[6, 7, 8]. In this paper we present a platform for generating a large volume of quiescent WDM plasma for use in stopping experiments, as in Ref. [6].

## 2. Experimental design

The OMEGA laser facility[9] was used to create both a source of protons and the subject plasma described in this work, as shown in Fig. 1. Using exploding pusher targets as a proton source is discussed in the literature[10, 6]. The WDM subject target consists of a tube coated with x-ray generating material, with a cylinder of the desired subject material inserted into the tube. The dimensions and materials depend on the experimental goal. In this first work, a plastic (CH)
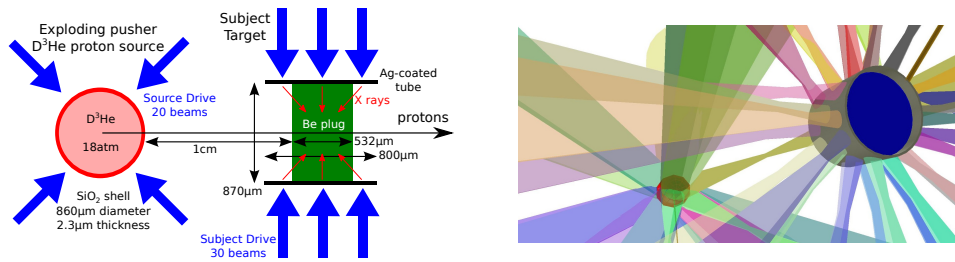
**Figure 1.** Experimental geometry: cartoon (left) and Visrad CAD model (right). A D$^3$He proton source, at left, creates protons to probe the subject plasma, at right, which is created by isochorically heating a solid plug with x rays.

tube coated with $1 - 2$ $\mu$m of Ag, with an inner diameter of $870\mu$m, a wall thickness of 24 $\mu$m, and 800 $\mu$m in length was used with a Be plug; for additional details see Ref. [6].

The arrangement of drive beams on the cylinder target must be chosen to optimally distribute the laser energy in the cylinder's azimuthal and axial directions. In this experiment, 30 OMEGA beams are available to heat the subject target. The chosen design arranges these beams into three rings of 10 beams each, which are pointed to achieve azimuthal symmetry. The three rings are displaced for axial symmetry. The chosen design is shown in Fig. 2, plotting the incident laser intensity versus $z$ and $\phi$ in the cylinder target's coordinate system.

Each beam is run without DPP and defocused to a $\sim 100$ $\mu$m diameter spot. The three rings are clearly visible at $z \sim -250$, 0, and 250 $\mu$m. The axial displacement for the first and last rings were chosen to match the Be plug dimensions (500 $\mu$m nominal total thickness). The final laser intensity in the spots is very high ($2 - 4 \times 10^{15}$ W/cm$^2$), which is desirable for generation of the Ag L-shell photons at 3-4keV in the corona surrounding the cylindrical target, which volumetrically heats the Be plug as the attenuation length in solid Be is $300 - 500$ $\mu$m, comparable to the cylinder's dimensions. The total drive energy was 15kJ in a 1ns square pulse.
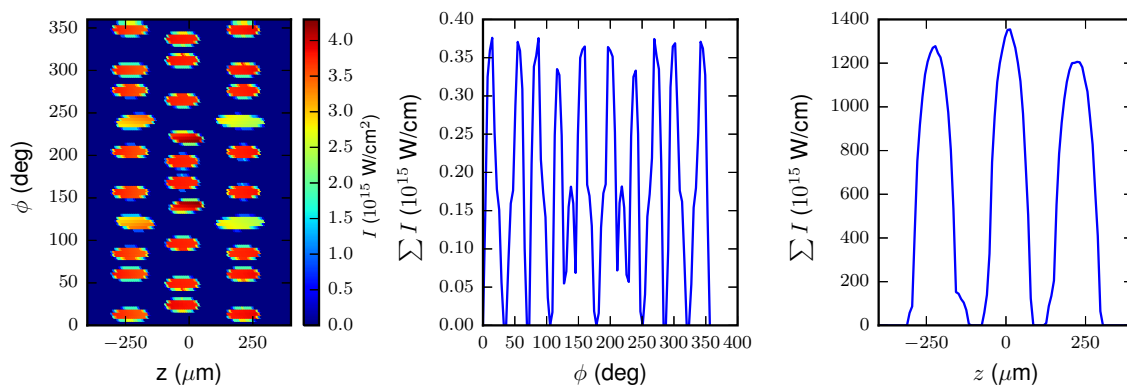


**Figure 2.** Laser drive used on the subject cylinder: surface intensity map (left), azimuthal energy distribution (center), and axial energy distribution (right).

## 3. X-ray characterization

Several instruments were used to diagnose the cylinder's x-ray emission. In particular, framing camera (XRFC) data and streaked spectrometer (SSCA) data were taken to qualitatively diagnose the spatial and temporal emission. The XRFC data is shown in Fig. 3. The emission in

time clearly lasts approximately 1ns, as expected from the laser drive. Early in time (top strip) the emission is dominated by the laser spots on the cylinder's surface. Later in time (strips 2 and 3) the emission region clearly increases, as the emission becomes more dominated by the hot coronal plasma surrounding the cylinder.
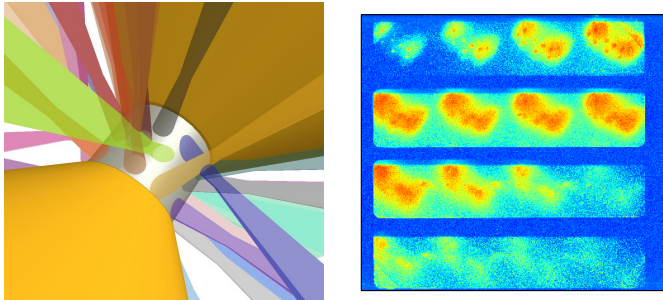


**Figure 3.** Left: XRFC view from TIM 1. Right: XRFC data as $\log I$ from shot 72016. A four-strip camera was used with 12× magnification. Time increases left to right and top to bottom. The time spanned by a single strip is 200ps, and the timing between strips is 400ps.

The SSCA data are shown in Fig. 4. In the raw data the energy dispersion direction is vertical, while time increases to the right (streak direction). This data can be qualitatively analyzed by looking at the emission profile in time of one of the bright lines, and looking at the spectrum for a single time in the middle of the pulse, as shown in the two plots in Fig. 4. The emission time history clearly shows that most of the Ag L-shell emission occurs early in the laser pulse. 1-D HYADES simulations indicate that the $1 - 2$ $\mu$m thick Ag layer burns through at around 0.5ns, corresponding to the rapid decrease in L-shell emission. It was expected that the coronal plasma would be hot enough to continue L-shell line emission, but the HYADES simulations suggest that the corona may be too hot - simulated electron temperatures reach $6 - 10$ keV towards the end of the pulse, which would mean that the Ag will be ionized to a He-like state. Future experiments could use a thicker Ag layer or a shorter laser pulse.
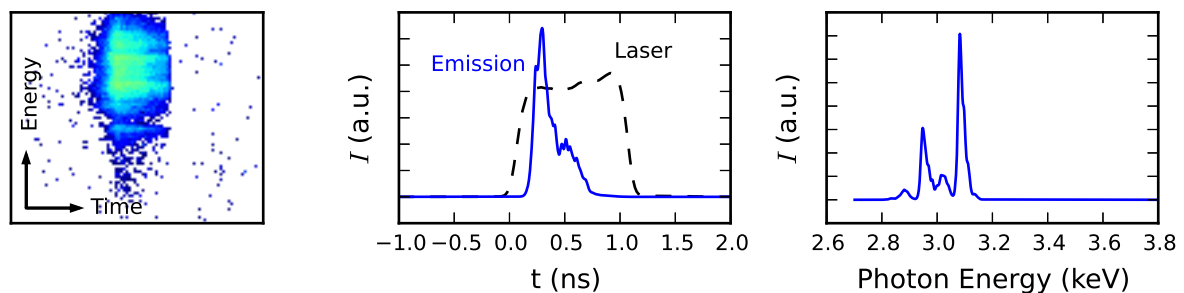


**Figure 4.** Left: Streaked spectrometer (SSCA) data from shot 72028 as background-subtracted $\log I$. Corresponding temporal emission profile (center) and time-snapshot spectrum (right) are plotted. The time and energy axes are only approximately calibrated, due to a lack of absolute calibration for this instrument.

## 4. Temperature measurements

Ideally the plasma conditions would be measured directly with a surrogate stopping power target. This was attempted with imaging x-ray Thomson scattering using the IXTS diagnostic[11]. We observed an unexpectedly high background originating from the cylinder heating, i.e. without the Thomson scattering x-ray source. This resulted in a very low signal-to-background in the scattering region, which precludes any interpretation of this data. Future experiments using this platform may be able to obtain high-quality x-ray Thomson scattering data by using better collimating shields. Another route that is being explored is dopant absorption spectroscopy.

## 5. Proton radiography

The implosion proton source was timed so that the proton probing occurs at 1.4 ns, which prevents target electrostatic charging effects[12] while preserving the temperature. The absence of target charging at the proton probing time was verified using proton radiography[10], as shown in Fig. 5. The expected view (left) is generated from a Visrad model of the experiment. Due to the use of larger implosion targets (see Fig. 1), the spatial resolution is degraded relative to standard D$^3$He proton backlighting[10]. However, the cylinder target with large $\rho L$ generates a central region without proton fluence, since protons transiting the cylinder are ranged out in the detector filtering. The expected cylinder size from geometric magnification is shown by the red dashed circle superimposed on the radiograph. The diameter of the image is consistent with the geometric magnification, demonstrating that field effects are not present. In the corona surrounding the driven cylinder, magnetic fields generated by the Biermann battery ($\nabla n \times \nabla T$) or laser-plasma interaction instabilities are present. While the electric charging of the target decays rapidly after the laser turns off[12], these magnetic fields can persist in the low-density coronal plasma, and show up in the radiograph as quasi-filamentary structures around the periphery of the image. These fields will not affect the stopping power measurement.
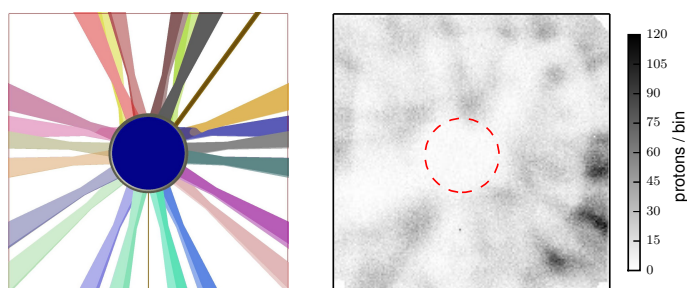


**Figure 5.** Proton radiography from shot 72028. Left: Radiography field of view from Visrad model, right: measured D$^3$He-p radiograph. The expected geometric size of the cylinder is shown by the red dashed circle.

## 6. Conclusion

A platform has been developed to generate a large volume of semi-quiescent WDM plasma, with a primary application being charged-particle stopping power experiments. 30 of the 60 OMEGA laser beams are used to drive a cylinder, which isochorically and indirectly heats the inner sample via high-energy x rays. X-ray diagnostics of the cylinder are presented showing that the spatial, temporal, and spectral characteristics of the drive are as expected. Finally, proton radiography is used to demonstrate that there are no electromagnetic fields impacting stopping-power measurements taken along the axis.

## References

[1] Ziegler J, Biersack J and Littmark U 1985 (Pergamon, New York)
[2] Trubnikov B 1965 *Particle Interactions in a Fully Ionized Plasma* (Consultant's Bureau)
[3] Li C and Petrasso R 1993 *Phys. Rev. Lett.* **70** 3059–3062
[4] Maynard G and Deutsch C 1985 *J. Physique* **46** 1113–1122
[5] L S Brown, D L Preston, and R L Singleton Jr 2005 *Physics Reports* **410** 237 – 333
[6] Zylstra A B *et al.* 2015 *Phys. Rev. Lett.* **114**(21) 215002
[7] Frenje J A *et al.* 2015 *Phys. Rev. Lett.* **115**(20) 205001
[8] Hayes A C *et al.* 2015 *Physics of Plasmas* **22** 082703
[9] Boehly T *et al.* 1997 *Optics Communications* **133** 495–506
[10] Li C K *et al.* 2006 *Rev. Sci. Instrum.* **77** 10E725
[11] Gamboa E J *et al.* 2012 *Rev. Sci. Instrum.* **83**(10) 10E108
[12] Hicks D G *et al.* 2000 *Phys. Plasmas* **7** 5106–5117